Chloroquine Resistance in *Plasmodium falciparum* Malaria Parasites Conferred by *pfcrt* Mutations

Amar Bir Singh Sidhu, Dominik Verdier-Pinard, David A. Fidock*

Plasmodium falciparum **chloroquine resistance is a major cause of worldwide increases in malaria mortality and morbidity. Recent laboratory and clinical studies have associated chloroquine resistance with point mutations in the gene *pfcrt*. However, direct proof of a causal relationship has remained elusive and most models have posited a multigenic basis of resistance. Here, we provide conclusive evidence that mutant haplotypes of the *pfcrt* gene product of Asian, African, or South American origin confer chloroquine resistance with characteristic verapamil reversibility and reduced chloroquine accumulation. *pfcrt* mutations increased susceptibility to artemisinin and quinine and minimally affected amodiaquine activity; hence, these antimalarials warrant further investigation as agents to control chloroquine-resistant *falciparum* malaria.**

Chloroquine has for decades been the primary chemotherapeutic means of malaria treatment and control (*1*). This safe and inexpensive 4-aminoquinoline compound accumulates inside the digestive vacuole of the infected red blood cell, where it is believed to form complexes with toxic heme moieties and interfere with detoxification mechanisms that include heme sequestration into an inert pigment called hemozoin (*2–4*). Chloroquine resistance (CQR) was first reported in Southeast Asia and South America and has now spread to the vast majority of malaria-endemic countries (*1*). *pfcrt* was recently identified as a candidate gene for CQR after the analysis of a genetic cross between a chloroquine-resistant clone (Dd2, Indochina) and a chloroquine-sensitive clone (HB3, Honduras) (*5–7*). The PfCRT protein localizes to the digestive vacuole membrane and contains 10 putative transmembrane domains (*7, 8*). Point mutations in PfCRT, including the $Lys^{76} \rightarrow Thr$ (K76T) mutation in the first predicted transmembrane domain, show an association with CQR in field isolates and clinical studies (*7, 9, 10*). Episomal complementation assays demonstrated a low-level, atypical CQR phenotype in chloroquine-selected, transformed, pseudo-diploid parasite lines that coexpressed the Dd2 form of *pfcrt* (containing eight point mutations; Table 1), under the control of a heterologous promoter, with the wild-type endogenous allele (*7*).

To address whether mutations in *pfcrt* are sufficient to confer CQR, we implemented an allelic exchange approach to replace the endogenous *pfcrt* allele of a chloroquine-sensitive line (GC03) with *pfcrt* alleles from chloroquine-resistant lines of Asian, African, or South American origin (Table 1) (fig. S1) (*11*). This approach maintained the endogenous promoter and terminator regulatory elements for correct stage-specific expression and did not use chloroquine during the selection procedure. As a result of this gene's highly interrupted nature (13 exons) and the dissemination of point mutations throughout the coding sequence, two rounds of genetic transformation were required. This enabled us to obtain *pfcrt*-modified clones that expressed the *pfcrt* allele from the chloroquine-resistant lines Dd2 (clones $C3^{Dd2}$ and $C4^{Dd2}$), K76I ($C5^{K76I}$), and 7G8 ($C6^{7G8}$). We also obtained the $C2^{GC03}$ clone in which recombination had occurred downstream of the functional allele, providing a critical control in correcting for any influence of inserting the two selectable marker cassettes without exchanging *pfcrt* point mutations (Table 1) (fig. S1).

pfcrt allelic exchange was confirmed by Southern hybridization and polymerase chain reaction (PCR) analysis (fig. S2, A to D, and table S1). Reverse-transcription PCR analysis confirmed transcription of the recombinant functional *pfcrt* allele (fig. S2C), whereas no transcription was observed from the downstream remnant *pfcrt* sequences that lacked a promoter and 5′ coding sequence. Western blot analysis (*7, 8*) revealed expression of PfCRT (about 42 kD) in all clones (fig. S2E). Quantitation analysis predicted a reduction in PfCRT expression of approximately 30 to 40%, 50%, and 0%, respectively, in the $C3^{Dd2}/C4^{Dd2}$, $C5^{K76I}$, and $C6^{7G8}$ clones, relative to $C2^{GC03}$, which itself expressed 30% less PfCRT than did the original GC03 clone (*11*).

Phenotypic analysis showed that mutant *pfcrt* alleles conferred a CQR phenotype to chloroquine-sensitive *P. falciparum* (Fig. 1A). Recombinant clones expressing *pfcrt* alleles from the chloroquine-resistant lines Dd2, K76I, and 7G8 all had 50% inhibitory concentration (IC_{50}) values in the range of 100 to 150 nM. These IC_{50} values were typically 70 to 90% of those observed with the nontransformed chloroquine-resistant lines. All these lines equaled or exceeded the 80 to 100 nM level previously proposed as a threshold diagnostic of in vivo resistant infections (*12, 13*). In comparison, chloroquine IC_{50} values in the recombinant control lines $C1^{GC03}$ and $C2^{GC03}$ were comparable to those observed with the initial GC03 line (20 to 30 nM). Acquisition of resistance was even more pronounced for the active metabolite monodesethylchloroquine, with IC_{50} values in the range of 600 to 1200 nM for the *pfcrt*-modified lines, versus 35 to 40 nM for chloroquine-sensitive lines (table S2).

The lower chloroquine IC_{50} values observed in the *pfcrt*-modified clones, relative to the nontransformed chloroquine-resistant lines, may be a consequence of the reduced PfCRT expression levels and other effects stemming from the complex genetic locus created in these recombinant clones (fig. S1). Alternatively, additional genetic factors might be required to attain high chloroquine IC_{50} values. One candidate secondary determinant is *pfmdr1*, which encodes the P-glycoprotein homolog Pgh-1 that localizes to the digestive vacuole (*14–16*). Reed *et al.* (*17*) recently demonstrated by allelic exchange that removal of three *pfmdr1* point mutations (1034C, 1042D, and 1246Y) from the 7G8 line decreased the chloroquine IC_{50} values; however, introduction of these mutations into endogenous *pfmdr1* did not alter the susceptible phenotype of a chloroquine-sensitive line. Our experiments were performed with the GC03 clone, which carries the HB3-type *pfmdr1* allele that in two *P. falciparum* genetic crosses showed no association with decreased chloroquine susceptibility (*5, 18*). This allele contains the 1042D point mutation that is prevalent in chloroquine-resistant South American isolates, although this mutation does not show a consistent association with CQR in isolates from other malaria-endemic regions (*6, 19–21*).

Acquisition of elevated chloroquine IC_{50} values in the *pfcrt*-modified clones was accompanied by verapamil chemosensitization, a hallmark of the CQR phenotype (Fig. 1A) (*22*). Association of both parameters with *pfcrt* represents a marked departure from earlier suppositions that verapamil reversibility of *P. falciparum* CQR was analogous to this compound's chemosensitization of multidrug resistance in mammalian tumor cells, believed to be mediated primarily by adenosine

Department of Microbiology and Immunology, Albert Einstein College of Medicine, Bronx, NY 10461, USA.

*To whom correspondence should be addressed. E-mail: dfidock@aecom.yu.edu

triphosphate–dependent P-glycoproteins (*22*). We note that verapamil reversibility was more pronounced in the clones expressing recombinant *pfcrt* from Old World (Dd2, K76I) origins than in the clone expressing the recombinant New World (7G8) allele. These findings are consistent with the recent report of reduced verapamil reversibility in chloroquine-resistant field isolates expressing the PfCRT 7G8 haplotype (*23*). In an independent confirmation of the CQR phenotype of *pfcrt*-modified clones, we observed significantly reduced [^{3}H]chloroquine accumulation in the C3^{Dd2}, Dd2, C6^{7G8}, and 7G8 clones as compared with the chloroquine-sensitive clones GC03 and C2^{GC03} (Fig. 1G). These assays measured the uptake into infected red blood cells of the saturable component of chloroquine at nanomolar concentrations, a measure that has been previously found to clearly distinguish chloroquine-resistant and chloroquine-sensitive parasites (*24, 25*).

Having this set of clones on the same genetic background, in which CQR was produced in vitro via modification of a single gene, allowed us to begin investigations into the relationship between *pfcrt*, CQR, and *P. falciparum* susceptibility to related antimalarials. We focused initially on amodiaquine, a chloroquine analog with the same aminoquinoline ring that differs by the presence of an aromatic ring in the side chain (fig. S3). Drug assays showed that the lines harboring mutant *pfcrt* were slightly less susceptible to

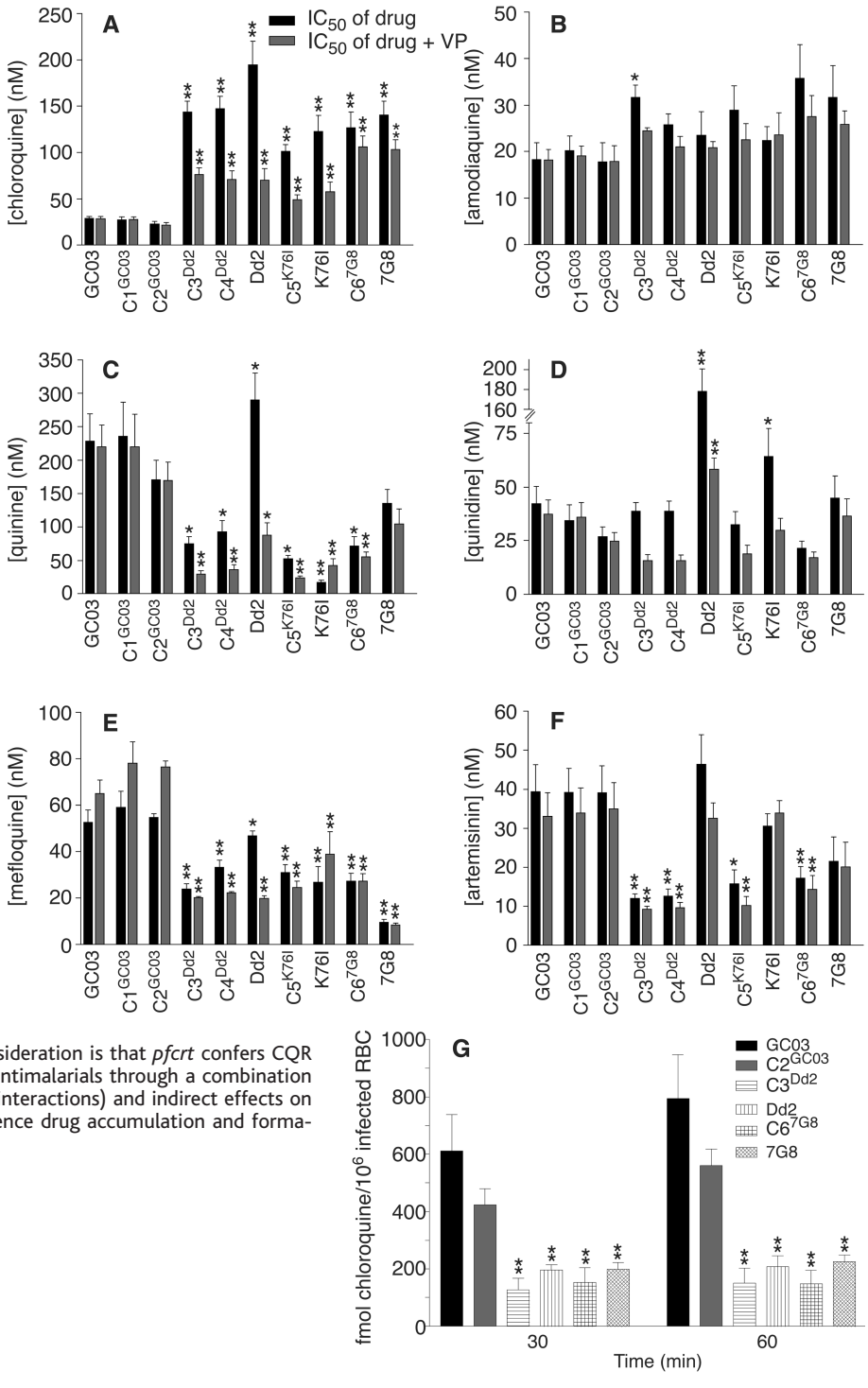

Fig. 1. *pfcrt* mutations confer chloroquine resistance and altered susceptibility to other heme (ferriprotoporphyrin IX)–binding antimalarials in *P. falciparum*. (**A** to **F**) Results of in vitro drug assays with *pfcrt*-modified and control lines. Each line was tested in duplicate against each antimalarial drug at least four times, in the presence or absence of 0.8 μM verapamil (VP). IC_{50} values (shown as the mean + SE for each line) correspond to the concentration at which incorporation of [^{3}H]hypoxanthine was half-maximal and were derived from the inhibition curves generated as a function of drug concentration. Mann-Whitney tests were used to assess statistically significant differences between the reference line C2^{GC03} and the others (*$P < 0.05$, **$P < 0.01$). IC_{50} and IC_{90} values and compound structures are detailed in table S2 and fig. S3. The finding that *pfcrt* mutations conferred increased susceptibility to both quinine and mefloquine provides an intriguing contrast with the recent report that the introduction of mutations into *pfmdr1* led to decreased susceptibility to quinine and increased susceptibility to mefloquine (*17*). (**G**) Chloroquine accumulation assays (using 30 nM [^{3}H]chloroquine) confirm that *pfcrt* mutations confer a CQR phenotype. The saturable component of [^{3}H]chloroquine accumulation, measured as femtomoles of drug per 10^6 infected red blood cells, was calculated by subtracting the nonsaturable accumulation (measured in the presence of 10 μM unlabeled chloroquine) from the total accumulation (measured in the absence of unlabeled drug). The mean + SE, calculated from five experiments performed in duplicate, is shown for each line. Accumulation values in the *pfcrt*-modified clones C3^{Dd2} and C6^{7G8} showed a statistically significant difference from values observed in C2^{GC03} (**$P < 0.01$). The chloroquine data in (A) and (G) prove a central role for *pfcrt* point mutations in conferring CQR to the GC03 line, although they do not rule out the possibility that other loci can contribute to this phenotype. It remains to be established whether mutant *pfcrt* alleles can confer CQR to multiple, genetically distinct chloroquine-sensitive lines. One hypothesis under consideration is that *pfcrt* confers CQR and altered susceptibility to other heme-binding antimalarials through a combination of direct effects (which may involve drug-protein interactions) and indirect effects on parasite physiological processes (which may influence drug accumulation and formation of drug-heme complexes).

Table 1. Transformation status and PfCRT haplotype of recombinant and wild-type lines. The first round of transformation (*11*) was performed with GC03 and used a plasmid containing the human dihydrofolate reductase (hDHFR) selectable marker (*40*). The resulting clone, $C1^{GC03}$ (fig. S1), shared the same chloroquine IC_{50} values (Fig. 1) (table S2) and *pfcrt* coding sequence as GC03. Transformation of $C1^{GC03}$ in the second round used plasmids containing the blasticidin S-deaminase (BSD) selectable marker (*41*) and resulted in the C2 to C6 clones. GC03 is a chloroquine-sensitive progeny of the genetic cross between the chloroquine-resistant clone Dd2 (Indochina) and the chloroquine-sensitive clone HB3 (Honduras) (*5, 6*). Dd2 and 7G8 (Brazil) represent common PfCRT haplotypes found in Asia/Africa and South America, respectively (*7*). K76I is a chloroquine-resistant line selected from the chloroquine-sensitive 106/1 (Sudan) clone propagated in the presence of high chloroquine concentrations, resulting in the generation of a full complement of PfCRT point mutations including the novel K76I mutation (*8*). Point mutations in boldface are those previously associated with CQR (*7, 8*). Abbreviations for amino acid residues: A, Ala; C, Cys; D, Asp; E, Glu; I, Ile; K, Lys; L, Leu; M, Met; N, Asn; Q, Gln; R, Arg; S, Ser; T, Thr.

Clone	First plasmid integration	Second plasmid integration	Change in PfCRT haplotype	Functional PfCRT haplotype								
				72	74	75	76	220	271	326	356	371
GC03	—	—	—	C	M	N	K	A	Q	N	I	R
$C1^{GC03}$	phDHFR-crt-$GC03^{Pf3'}$	—	No	C	M	N	K	A	Q	N	I	R
$C2^{GC03}$	phDHFR-crt-$GC03^{Pf3'}$	pBSD-crt-$Dd2^{Py3'}$	No	C	M	N	K	A	Q	N	I	R
$C3^{Dd2}$	phDHFR-crt-$GC03^{Pf3'}$	pBSD-crt-$Dd2^{Pf3'}$	Yes	C	**I**	**E**	**T**	**S**	**E**	**S**	**T**	**I**
$C4^{Dd2}$	phDHFR-crt-$GC03^{Pf3'}$	pBSD-crt-$Dd2^{Py3'}$	Yes	C	**I**	**E**	**T**	**S**	**E**	**S**	**T**	**I**
Dd2	—	—	—	C	**I**	**E**	**T**	**S**	**E**	**S**	**T**	**I**
$C5^{K76I}$	phDHFR-crt-$GC03^{Pf3'}$	pBSD-crt-K76I$^{Pf3'}$	Yes	C	**I**	**E**	**I**	**S**	**E**	**S**	I	**I**
K76I	—	—	—	C	**I**	**E**	**I**	**S**	**E**	**S**	I	**I**
$C6^{7G8}$	phDHFR-crt-$GC03^{Pf3'}$	pBSD-crt-$7G8^{Py3'}$	Yes	**S**	M	N	**T**	**S**	Q	**D**	**L**	R
7G8	—	—	—	**S**	M	N	**T**	**S**	Q	**D**	**L**	R

amodiaquine (Fig. 1B); nonetheless, the *pfcrt*-modified clones remained sensitive to this drug, with IC_{50} values of 22 to 36 nM. A modest degree of cross-resistance was observed between chloroquine and monodesethylamodiaquine, the primary metabolite of amodiaquine (table S2) (*26–28*). These findings are consistent with the published data on amodiaquine efficacy in areas with a high prevalence of CQR malaria (*29, 30*) and signal the need for close monitoring for resistance, including screening for possible additional changes in *pfcrt* sequence, with increased clinical use of amodiaquine. Further, these data suggest that CQR mediated by *pfcrt* point mutations now prevalent in endemic areas has a high degree of specificity for the chloroquine structure (fig. S3). Other groups have reported that altering the chloroquine side chain length can result in a gain of efficacy against chloroquine-resistant lines (*31, 32*).

Phenotypic characterization also revealed increased susceptibility (by a factor of 2 to 4) to quinine, mefloquine, and artemisinin and its metabolite dihydroartemisinin in the *pfcrt*-modified clones (Fig. 1, C, E, and F) (table S2). These data provide direct evidence for an important role for this gene in determining parasite susceptibility to these antimalarials. Collateral hypersensitivity to these compounds is reminiscent of antimalarial susceptibility patterns observed in a Thailand study of *P. falciparum* field isolates (*33*) and is encouraging given their current clinical usage in antimalarial combination therapy regimes (*34*). In comparison to $C2^{GC03}$, the Dd2 line is more quinine resistant; however, the introduction of the Dd2 *pfcrt* allele (resulting in the clones $C3^{Dd2}$ and $C4^{Dd2}$) conferred quinine susceptibility (Fig. 1C). This implicates *pfcrt* as a component of a multifactorial process that governs parasite susceptibility to these antimalarials. Upon introduction of *pfcrt* point mutations, the increased susceptibility to quinine was accompanied by a decrease in susceptibility to the diastereomer quinidine (Fig. 1, C and D).

These data, obtained in lines that were not exposed to chloroquine pressure during their selection, agree with an earlier observation on the chloroquine-selected K76I line (*7, 8*) and suggest a structure-specific component of PfCRT-mediated drug accumulation in the digestive vacuole. All of these compounds are believed to act, at least in part, by complexing with heme products (*35, 36*). Possibly, PfCRT mutations affect accumulation by altering drug flux across the digestive vacuole membrane. Our data also document a key role for *pfcrt* point mutations in the mode of action of verapamil, a known CQR reversal agent (*22, 25, 37, 38*) that also chemosensitized the *pfcrt*-modified lines to quinine and quinidine (Fig. 1, C and D). This verapamil-reversible phenotype may reflect a physical association between verapamil and mutant PfCRT and/or mutant PfCRT-mediated physiological changes that alter the activity of verapamil on heme processing and drug-hematin binding. Our genetic system now provides a direct means to evaluate the precise role of individual *pfcrt* point mutations in determining *P. falciparum* drug response and verapamil reversibility, via site-directed mutagenesis and introduction of mutant alleles into chloroquine-sensitive lines.

These data are consistent with the concept that the appearance of *pfcrt* mutant alleles in a limited number of foci was the pivotal driving force behind the genesis and spread of CQR worldwide. The structural specificity of this *pfcrt*-mediated resistance mechanism is underscored by the finding that *pfcrt*-modified clones remained susceptible to amodiaquine, promoting the use of this and related compounds that differ in their aminoquinoline side chain for the treatment of chloroquine-resistant *falciparum* malaria. Identification of PfCRT as the major component of CQR and an important determinant of susceptibility to other heme-binding antimalarials offers alternative strategies for targeting the hemoglobin detoxification pathway for malaria treatment and control.

Note added in proof: Wootton *et al*. (*39*) recently presented compelling evidence for rapid evolutionary sweeps of mutant *pfcrt* sequences throughout malaria-endemic areas, starting from a limited number of initial foci. These sweeps presumably occurred as a result of intense chloroquine pressure. These data complement and support our finding that mutant *pfcrt* sequences from different continents can confer CQR to chloroquine-sensitive parasites.

References and Notes

1. R. G. Ridley, *Nature* **415**, 686 (2002).
2. D. J. Sullivan Jr., H. Matile, R. G. Ridley, D. E. Goldberg, *J. Biol. Chem.* **273**, 31103 (1998).
3. S. Pagola, P. W. Stephens, D. S. Bohle, A. D. Kosar, S. K. Madsen, *Nature* **404**, 307 (2000).
4. H. Ginsburg, S. A. Ward, P. G. Bray, *Parasitol. Today* **15**, 357 (1999).
5. T. E. Wellems *et al*., *Nature* **345**, 253 (1990).
6. X.-z. Su, L. S. Kirkman, T. E. Wellems, *Cell* **91**, 593 (1997).
7. D. A. Fidock *et al*., *Mol. Cell* **6**, 861 (2000).
8. R. A. Cooper *et al*., *Mol. Pharmacol.* **61**, 35 (2002).
9. A. Djimdé *et al*., *N. Engl. J. Med.* **344**, 257 (2001).
10. T. E. Wellems, C. V. Plowe, *J. Infect. Dis.* **184**, 170 (2001).
11. See supporting data on *Science* Online.
12. P. Brasseur, J. Kouamouo, R. Moyou-Somo, P. Druilhe, *Am. J. Trop. Med. Hyg.* **46**, 1 (1992).
13. G. Cremer, L. K. Basco, J. Le Bras, D. Camus, C. Slomianny, *Exp. Parasitol.* **81**, 1 (1995).
14. S. J. Foote, J. K. Thompson, A. F. Cowman, D. J. Kemp, *Cell* **57**, 921 (1989).
15. C. M. Wilson *et al*., *Science* **244**, 1184 (1989).

16. A. F. Cowman, S. Karcz, D. Galatis, J. G. Culvenor, *J. Cell Biol.* **113**, 1033 (1991).
17. M. B. Reed, K. J. Saliba, S. R. Caruana, K. Kirk, A. F. Cowman, *Nature* **403**, 906 (2000).
18. M. T. Duraisingh, C. Roper, D. Walliker, D. C. Warhurst, *Mol. Microbiol.* **36**, 955 (2000).
19. S. J. Foote *et al.*, *Nature* **345**, 255 (1990).
20. L. K. Basco, J. Le Bras, Z. Rhoades, C. M. Wilson, *Mol. Biochem. Parasitol.* **74**, 157 (1995).
21. S. C. Chaiyaroj, A. Buranakiti, P. Angkasekwinai, S. Looressuwan, A. F. Cowman, *Am. J. Trop. Med. Hyg.* **61**, 780 (1999).
22. S. K. Martin, A. M. Oduola, W. K. Milhous, *Science* **235**, 899 (1987).
23. R. K. Mehlotra *et al.*, *Proc. Natl. Acad. Sci. U.S.A.* **98**, 12689 (2001).
24. D. J. Krogstad, I. Y. Gluzman, B. L. Herwaldt, P. H. Schlesinger, T. E. Wellems, *Biochem. Pharmacol.* **43**, 57 (1992).
25. P. G. Bray, M. Mungthin, R. G. Ridley, S. A. Ward, *Mol. Pharmacol.* **54**, 170 (1998).
26. G. E. Childs *et al.*, *Am. J. Trop. Med. Hyg.* **40**, 7 (1989).
27. L. K. Basco, J. Le Bras, *Am. J. Trop. Med. Hyg.* **48**, 120 (1993).
28. P. G. Bray, S. R. Hawley, M. Mungthin, S. A. Ward, *Mol. Pharmacol.* **50**, 1559 (1996).
29. P. Olliaro *et al.*, *Lancet* **348**, 1196 (1996).
30. M. Adjuik *et al.*, *Lancet* **359**, 1365 (2002).
31. D. De, F. M. Krogstad, F. B. Cogswell, D. J. Krogstad, *Am. J. Trop. Med. Hyg.* **55**, 579 (1996).
32. R. G. Ridley *et al.*, *Antimicrob. Agents Chemother.* **40**, 1846 (1996).
33. R. N. Price *et al.*, *Antimicrob. Agents Chemother.* **43**, 2943 (1999).
34. N. J. White, *Parassitologia* **41**, 301 (1999).
35. M. Foley, L. Tilley, *Pharmacol. Ther.* **79**, 55 (1998).
36. P. M. O'Neill, P. G. Bray, S. R. Hawley, S. A. Ward, B. K. Park, *Pharmacol. Ther.* **77**, 29 (1998).
37. D. J. Krogstad *et al.*, *Science* **238**, 1283 (1987).
38. L. M. B. Ursos, S. Dzekunov, P. D. Roepe, *Mol. Biochem. Parasitol.* **110**, 125 (2000).
39. J. C. Wootton *et al.*, *Nature* **418**, 320 (2002).
40. D. A. Fidock, T. E. Wellems, *Proc. Natl. Acad. Sci. U.S.A.* **94**, 10931 (1997).
41. C. B. Mamoun, I. Y. Gluzman, S. Goyard, S. M. Beverley, D. E. Goldberg, *Proc. Natl. Acad. Sci. U.S.A.* **96**, 8716 (1999).

42. We thank T. Wellems, P. Roepe, and S. Krishna for many helpful discussions. We also thank A. Talley, R. Cooper, D. Jacobus, S. Ward, P. Bray, W. Ellis, P. Ringwald, and N. Shulman. Supported by National Institute of Allergy and Infectious Diseases grant R01 AI50234, the Speaker's Fund for Biomedical Research, a New Scholar Award in Global Infectious Disease from the Ellison Medical Foundation, and the Howard Hughes Medical Institute Research Resources Program for Medical Schools.

Supporting Online Material
www.sciencemag.org/cgi/content/full/298/5591/210/DC1
Materials and Methods
Figs. S1 to S3
Tables S1 and S2

16 May 2002; accepted 5 August 2002

Genetic Loci Affecting Resistance to Human Malaria Parasites in a West African Mosquito Vector Population

Oumou Niaré,[1,2]* Kyriacos Markianos,[3]* Jennifer Volz,[5]* Frederick Oduol,[1] Abdoulaye Touré,[2] Magaran Bagayoko,[2] Djibril Sangaré,[2] Sekou F. Traoré,[2] Rui Wang,[5] Claudia Blass,[5] Guimogo Dolo,[2] Madama Bouaré,[2] Fotis C. Kafatos,[5] Leonid Kruglyak,[3,4] Yeya T. Touré,[2] Kenneth D. Vernick[1]†

Successful propagation of the malaria parasite *Plasmodium falciparum* within a susceptible mosquito vector is a prerequisite for the transmission of malaria. A field-based genetic analysis of the major human malaria vector, *Anopheles gambiae*, has revealed natural factors that reduce the transmission of *P. falciparum*. Differences in *P. falciparum* oocyst numbers between mosquito isofemale families fed on the same infected blood indicated a large genetic component affecting resistance to the parasite, and genome-wide scanning in pedigrees of wild mosquitoes detected segregating resistance alleles. The apparently high natural frequency of resistance alleles suggests that malaria parasites (or a similar pathogen) exert a significant selective pressure on vector populations.

Mosquitoes infected with malaria incur quantifiable costs in reproductive fitness for measures such as longevity, fecundity, and flight distance (*1*–*3*). In addition, mosquito immune genes respond transcriptionally to malaria parasite infection (*4*–*6*), indicating that malaria parasites are detected by mosquito immune surveillance. Inbred lines selected from mosquito colonies can inhibit parasite development through at least two distinct mechanisms: melanotic encapsulation and intracellular lysis (*7*, *8*). Therefore, selective pressure by parasite infection could drive the natural selection of resistance mechanisms in mosquitoes. However, previous studies of resistance used laboratory strains of mosquitoes and malaria parasites, which are known to display biological aberrations in comparison to natural populations (*9*–*11*), and thus the relevance of these studies to natural malaria transmission may be questioned. Malaria resistance mechanisms and their significance for the biology of malaria transmission have not been examined previously in natural field populations of vectors.

For study of the vector-parasite interaction using field populations, standard genetic techniques that require the creation of inbred or isogenic lines were not applicable. However, the large number of progeny produced by single wild females permitted a novel study design based on isofemale pedigrees, which is quite distinct from designs previously used in human and animal genetics (fig. S1). In nature, *A. gambiae* females mate only once (*12*), and the stored sperm is used to fertilize successive egg batches that mature when the female feeds on blood. We captured pre-mated blood-fed females resting in village dwellings in Bancoumana, Mali (West Africa); allowed them to oviposit in an environmentally controlled chamber; and then raised their respective progeny in the environmental chamber (*13*). We used the isofemale families at either the F_1 or the F_2 stage (the latter produced by mass mating of F_1 mosquitoes). All females of a family were challenged with malaria parasites by being fed on blood from the same *P. falciparum* gametocyte carrier (*14*). Unfed mosquitoes were removed (*15*). At 8 days after infection, the progeny were dissected, and the surviving oocyst-stage parasites were counted in each midgut. The number of oocysts per mosquito constituted the quantitative infection phenotype.

We investigated the genetic dependence of mosquito resistance to malaria infection in two stages. First, in a familiality study, we compared parasite infection levels between mosquito families that were each generated by a different founding pair of wild mosquitoes. The goal was to measure interfamily differences in infection distributions, and therefore only phenotype measurements were used. Groups of three F_1 families were reared together in an environmental chamber and were fed simultaneously on blood from a

[1]Department of Medical and Molecular Parasitology, New York University School of Medicine, 341 East 25th Street, New York, NY 10010, USA. [2]Département d'Epidémiologie des Affectations Parasitaires, Faculté de Médecine, de Pharmacie et d'Odonto-Stomatologie, Boite Postale 1805, Bamako, Mali. [3]Fred Hutchinson Cancer Research Center, 1100 Fairview Avenue North, Seattle, WA 98109, USA. [4]Howard Hughes Medical Institute, 4000 Jones Bridge Road, Chevy Chase, MD 20815, USA. [5]European Molecular Biology Laboratories, Meyerhofstrasse 1, 69117 Heidelberg, Germany.

*These authors contributed equally to this work.
†To whom correspondence should be addressed. E-mail: kenneth.vernick@nyu.edu

Supplemental Materials and Methods and Figures for A. B. S. Sidhu, D. Verdier-Pinard, D. A. Fidock: *pfcrt* Mutations Confer Chloroquine Resistance to *Plasmodium falciparum* Malaria Parasites.

Parasite transfection. *P. falciparum* parasite lines were propagated in human red blood cells (RBC) in RPMI medium supplemented with 0.5% Albumax and were electroporated with purified plasmid DNA, as described *(S1)*. Transformed parasites were selected using 5 nM WR99210 and 5 μM Blasticidin HCl (Invitrogen) to select for the human dihydrofolate reductase (hDHFR) and blasticidin S-deaminase (BSD) selectable markers, respectively *(S1, S2)*. Episomal transformation was quantified by plasmid rescue *(S3)*.

Nucleic acid and protein analysis. *P. falciparum* genomic DNA was purified using the $NaClO_4$ method *(S3, S4)*. Total RNA was isolated using the Qiagen RNeasy kit and residual DNA contamination was removed by DNase I treatment. cDNA was synthesized from total RNA using oligo (dT) priming and Superscript-II reverse transcriptase (Invitrogen). Tests for genomic DNA contamination were performed in parallel with mock cDNA reaction samples lacking reverse transcriptase.

Southern hybridizations were performed with hexamer-primed [^{32}P]-labeled DNA probed against 0.5–2.0 μg of genomic DNA per lane. The *pfcrt* exon 2-specific probe (340 bp) was PCR amplified from *P. falciparum* GCO3 and Dd2 genomic DNA using the primers 5'-AGATGGCTCACGTTTAGGTGGAGG and 5'-GTAATGTTTTATATTGGTAGGTGG. The pBluescript probe was generated from linearized plasmid DNA. Hybridization of Sal I + Cla I digested genomic DNA preparations with the *pfcrt* exon 2 probe demonstrated replacement of the 9.4 kb band in GC03 with 16.3/8.0/1.2 kb and 16.3/8.0/7.7/1.2 kb fragments in $C3^{Dd2}/C5^{K76I}$ and $C4^{Dd2}/C6^{7G8}$, respectively (Fig. S2A). The control $C2^{GC03}$ clone gave 15.9/8.0/1.2 kb bands consistent with integration of a single BSD plasmid downstream of the functional chloroquine-sensitive (CQS)-associated *pfcrt* allele. This interpretation was supported by the results of hybridization with pBluescript plasmid, which detected the same bands except for the 1.2 kb internal *pfcrt* fragment (Fig. S2B). A schematic representation of the *pfcrt* locus in the recombinant and control lines is shown in Fig. S1.

Protein samples were prepared from parasites (enriched in late ring and early trophozoite stages) that had been saponin-lysed, washed with 1 × PBS and denatured in Laemmli buffer. Protein from 5.0 x 10^6 parasites was loaded per well, electrophoresed on a 10% SDS-PAGE gel, and electroblotted onto PVDF membranes (Bio-Rad). Membranes were probed with affinity-purified rabbit anti-PfCRT antibody (diluted 1:200) *(S5)*, followed by incubation with horseradish peroxidase-conjugated goat anti-rabbit IgG (diluted 1:25,0000; Amersham Biosciences) and enhanced chemiluminescence detection. Protein loadings were normalized by four pilot gel migration and transfer assays involving detection of total protein by Coomassie blue staining of parallel gels and quantitation analysis of Western blots probed with rabbit polyclonal anti-STARP

antibody as an independent loading control *(S6)*. Densitometric analysis of autoradiograph data was performed using NIH Image v1.6.2 (http://rsb.info.nih.gov/nih-image/).

DNA constructs, mutagenesis and luciferase assays. *pfcrt* modular fragments were assembled from three contiguous sequences. The first sequence, denoted Δ1 (corresponding to nucleotides 23553–23757 of the GenBank accession number AF030694), spanned the middle of exon 1 to the intron 1/exon 2 junction. This was PCR amplified as a 229 bp fragment from Dd2 genomic DNA using the primers 5'-caagcggccgc**TGA**GAATTAGATAATTTAGTACAAGAA-GGAA (Not I site underlined, 5' in-frame stop codon in boldface) and 5'-cacctaggCGTGAGCCATCTGTTAAGGTC (Avr II restriction site underlined). This fragment was subcloned into pCR2.1 (Invitrogen) and the Sal I site in intron 1 was removed by replacing the internal Sal I + Avr II fragment with a double-stranded adaptor made by annealing the primers 5'-TCGAGCTTAACAGATGGCTCACGC and 5'-CTAGGCGTGAGCCATCTGTTAAGC (point mutation leading to loss of Sal I site is underlined).

The second sequence, denoted exons 2-13 (corresponding to nucleotides 23764–26533), was PCR amplified as a 1162 bp fragment from oligo (dT) primed cDNA of Dd2, 7G8 and GC03 using the primers 5'-acgcctaggTGGAGGTTCTTGTCTTGGTA and 5'-tgagtcgacGTTGGTTAA-TTCTCCTTC (Avr II and Sal I restriction sites underlined). The K76I insert was generated from the Dd2 exons 2-13 fragment following site-directed mutagenesis (Quikchange, Stratagene) with the primers 5'-GTGTATGTGTAATTGAAATAATTTTTGCTAAAAGAAC and 5'-GTTCTTTTAGCAAAAATTATTTCAATTACACATACAC (mutagenized codon 76 position underlined).

The third sequence, denoted Pf3' (corresponding to nucleotides 26540–27590) was PCR amplified as a 1069 bp fragment from the Dd2 *pfcrt* 3' UTR region with the primers 5'-aacgtcgacTCAATTATTACACAA**TAA**AAATATATC (Sal I site underlined, stop codon in boldface) and 5'-gaaggatccTAACTAAACTTGAAATAAGTGGCG (BamH I restriction site underlined). Exons 2-13 and Pf3' products were cloned into the pGEM-T vector (Promega). All inserts were sequenced on both strands to identify error-free clones. Inserts Δ1, exons 2-13 and Pf3' were ligated together using their cohesive ends and subcloned as a 2431 bp Not I + BamH I fragment into the 5.7 kb plasmids pHDWT *(S1)* and pCBM-BSD *(S2)*. These plasmids express hDHFR and BSD under the control of the *P. falciparum hrp3* 5' UTR and *hrp2* 3' UTR regulatory elements.

To increase the frequency of single-site crossover events at the 5' end of the *pfcrt* fragment upstream of codons 72–76, we replaced the 1.0 kb Pf3' fragment with a 0.7 kb fragment, denoted Py3', from the 3' UTR region of the *P. yoelii* rodent ortholog *pycg10* (A. B. S. Sidhu and D. Fidock, unpublished data; *S7*). Py3' was amplified using the primers 5'-acgtcgac-**TCAATTATTACACAATAA**ATATTTTTTTTAAATGCCAC (HPLC-purified, Sal I site underlined; boldface letters represent *pfcrt* exon 13 sequence up to the stop codon, remainder is from the *pycg10* locus) and 5'-caggatccTATTTCAAAAATCTTAGCATAAGG (BamH I site underlined). This fragment was cloned into all pBSD-based constructs. Both the Pf3' and Py3' fragments were confirmed to be functional in transient transfection luciferase assays using pHLH-1-

derived constructs containing these fragments in place of the *hrp2* 3'UTR sequence *(S8)*. Controlled duplicate experiments performed three times by DNA preloading of uninfected RBC *(S9)* demonstrated luciferase activities averaging 59% of those obtained with pHLH-1, with no significant differences in activity between Pf3' and Py3' (data not shown). Electroporations were performed on days zero and two, and parasites were harvested on day three by saponin lysis. Luciferase activities were measured in 1X luciferase reporter lysis buffer (Promega) on an auto-injector luminometer (Autolumat LB953, EG&G Berthold, Perkin Elmer).

PCR-based detection of allelic exchange events and parasite cloning. Parasite lines episomally transformed with the *pfcrt* allelic exchange constructs were PCR screened every month for integration events occurring as a result of homologous recombination and single-site crossover. Because all three *P. falciparum* fragments (*pfcrt*, *hrp3* and *hrp2*) in the transformation plasmids represented potential sites of integration, these were separately screened for integration. *pfcrt* integration was tested using PCR primer combinations listed in Table S1 (separate file). The presence of human *dhfr* was confirmed using the primers 5'-ATGCATGGTTCGCTAAACTGCATCG and 5'-AAGCTTAATCATTCTTC-TCATATACTTC (producing a 0.57 kb fragment). The primer combinations 5'-TAATACGACTCACTATAGGG + 5'-AACAAGTTATTGTTAAATTCGGAG and 5'-CACGAAGCCGCCACACATTGCC + CAAAGGAGCAAACAATTTTGTC were used to screen for integration into *hrp3* (resulting in a 2.19 kb band) and *hrp2* (producing a 1.02 kb band) respectively.

Mutation-specific PCR screening for exchange of point mutations in codons 72–76 was performed using the primers 5'-GTTCTTTTAGCAAAAATTGTTTCA (Dd2) or 5'-GTTCTTTTAGCAAAAATTTTATTC (GC03), combined with the ubiquitous primer 5'-AATTTCTTACATATAACAAAATGAAATTCGCAAGT. PCR products were sequenced using internal primers. In some instances, strategies to detect rare integration events were facilitated by the loss of a Sal I site in intron 1 and the introduction of novel Avr II and Sal I sites into exons 2 and 13, respectively (none of these changes altered the coding sequence). The proportion in each transformed line of parasites that had undergone *pfcrt* allelic exchange was estimated by comparing yields of recombinant and wild-type PCR products obtained with several genomic DNA dilutions and primer pairs. Parasites were cloned by limiting dilution (up to 3 series, with a maximum first series of 10^3 infected RBC per well and a last series at 0.25 infected RBC per well) in 96-well tissue culture plates. Clones were detected using the *P. falciparum* lactate dehydrogenase-specific Malstat™ assay *(S10)*.

In vitro antimalarial drug assays. The response to antimalarial drugs was measured in vitro using 72 hr [^{3}H]-hypoxanthine assays in 96-well plates, starting with an initial parasitemia of 0.4%–0.5% *(S1, S11)*. The percentage reduction in [^{3}H]-hypoxanthine incorporation, a standard marker of parasite growth inhibition, was equal to:

$$100 \times \left(\frac{\text{(geometric mean cpm of wells without drug) - (mean cpm of test wells)}}{\text{(geometric mean cpm of wells without drug)}} \right)$$

IC_{50} and IC_{90} values were determined by regression analysis and curve fittings. Both the unpaired Student's *t* test and the Mann-Whitney test were performed for all comparisons between lines and the latter, more stringent test was used for data presentation. In vitro data and chemical structures are shown in Table S2 (see separate file) and Fig. S3 (see below).

Chloroquine accumulation analysis. *P. falciparum* parasites were sorbitol-synchronized and assayed at 2–8% parasitemia, 75-85% early to mid-stage trophozoites and 2–3% hematocrit. [^{3}H]-labeled chloroquine (specific activity 5 Ci/mmol, American Radiolabeled Chemicals) was added to duplicate samples (each at 0.3 ml of culture) at a final concentration of 30 nM. This value is close to the IC_{50} value of the CQS clones (Table S2). Assays were carried out in RPMI medium (containing $NaHCO_3$) for up to 60 minutes at 37°C in 24-well plates placed in humid chambers gassed with 5% O_2 / 5% CO_2 / 90% N_2. Samples were then centrifuged through silicon oil (d = 1.050, Aldrich) to separate the RBC pellet from unincorporated label, and the pellets and supernatants processed as described *(S12-S14)*. Control samples included uninfected RBC and infected RBC in which the [^{3}H]-chloroquine was added along with 10 μM unlabeled chloroquine. Statistical significance was examined using Mann-Whitney tests.

References and Notes

S1. D. A. Fidock, T. Nomura, T. E. Wellems, *Mol. Pharmacol.* **54**, 1140 (1998).

S2. C. B. Mamoun, I. Y. Gluzman, S. Goyard, S. M. Beverley, D. E. Goldberg, *Proc. Natl. Acad. Sci. U.S.A.* **96**, 8716 (1999).

S3. D. A. Fidock, T. E. Wellems, *Proc. Natl. Acad. Sci. U.S.A.* **94**, 10931 (1997).

S4. T. E. Wellems *et al.*, *Cell* **49**, 633 (1987).

S5. D. A. Fidock *et al.*, *Mol. Cell* **6**, 861 (2000).

S6. D. A. Fidock *et al.*, *Mol. Biochem. Parasitol.* **64**, 219 (1994).

S7. Preliminary sequence data from the *P. yoelii* genome was obtained from The Institute for Genomic Research website (www.tigr.org). This sequencing program is carried on in collaboration with the Naval Medical Research Center and is supported by the U.S. Department of Defense.

S8. Y. Wu, C. D. Sifri, H. H. Lei, X. Z. Su, T. E. Wellems, *Proc. Natl. Acad. Sci. U.S.A.* **92**, 973 (1995).

S9. K. Deitsch, C. Driskill, T. Wellems, *Nucleic Acids Res.* **29**, 850 (2001).

S10. I. D. Goodyer, T. F. Taraschi, *Exp. Parasitol.* **86**, 158 (1997).

S11. R. E. Desjardins, C. J. Canfield, J. D. Haynes, J. D. Chulay, *Antimicrob. Agents Chemother.* **16**, 710 (1979).

S12. D. J. Krogstad, I. Y. Gluzman, B. L. Herwaldt, P. H. Schlesinger, T. E. Wellems, *Biochem. Pharmacol.* **43**, 57 (1992).

S13. J. A. Martiney, A. Cerami, A. F. Slater, *J. Biol. Chem.* **270**, 22393 (1995).

S14. P. G. Bray, M. Mungthin, R. G. Ridley, S. A. Ward, *Mol. Pharmacol.* **54**, 170 (1998).

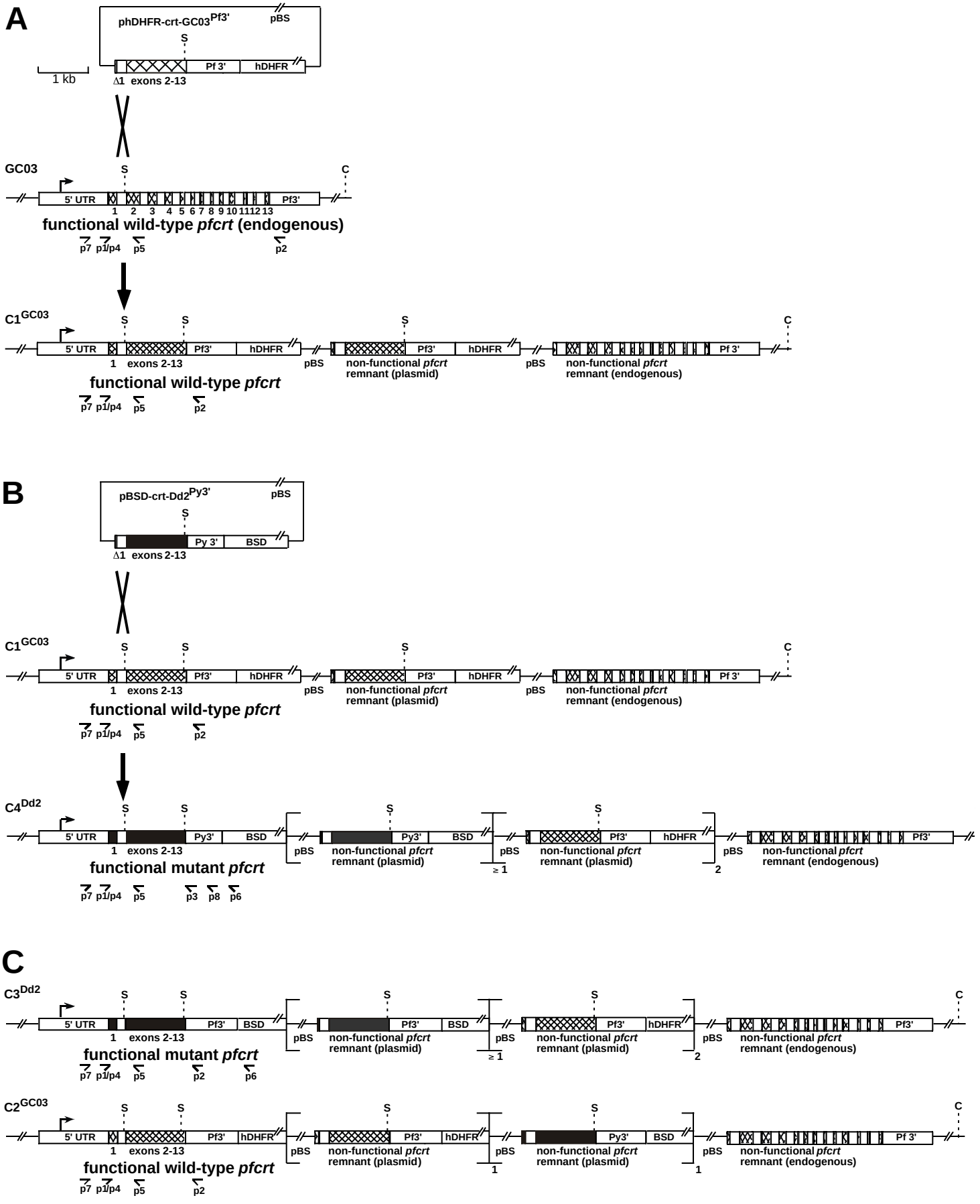
A
phDHFR-crt-GC03Pf3'
pBS
S
Pf 3'
hDHFR
1 kb
Δ1 exons 2-13
GC03
S
C
5' UTR
Pf3'
1 2 3 4 5 6 7 8 9 10 11 12 13
functional wild-type pfcrt (endogenous)
p7 p1/p4 p5 p2
C1GC03
S S S C
5' UTR
Pf3'
hDHFR
Pf3'
hDHFR
Pf 3'
1 exons 2-13
pBS
non-functional pfcrt remnant (plasmid)
pBS
non-functional pfcrt remnant (endogenous)
functional wild-type pfcrt
p7 p1/p4 p5 p2
B
pBSD-crt-Dd2Py3'
pBS
S
Py 3'
BSD
Δ1 exons 2-13
C1GC03
S S S C
5' UTR
Pf3'
hDHFR
Pf3'
hDHFR
Pf 3'
1 exons 2-13
pBS
non-functional pfcrt remnant (plasmid)
pBS
non-functional pfcrt remnant (endogenous)
functional wild-type pfcrt
p7 p1/p4 p5 p2
C4Dd2
S S S S S C
5' UTR
Py3'
BSD
Py3'
BSD
Pf3'
hDHFR
Pf3'
1 exons 2-13
pBS
non-functional pfcrt remnant (plasmid)
≥ 1
pBS
non-functional pfcrt remnant (plasmid)
2
pBS
non-functional pfcrt remnant (endogenous)
functional mutant pfcrt
p7 p1/p4 p5 p3 p8 p6
C
C3Dd2
S S S S C
5' UTR
Pf3'
BSD
Pf3'
BSD
Pf3'
hDHFR
Pf3'
1 exons 2-13
pBS
non-functional pfcrt remnant (plasmid)
≥ 1
pBS
non-functional pfcrt remnant (plasmid)
2
pBS
non-functional pfcrt remnant (endogenous)
functional mutant pfcrt
p7 p1/p4 p5 p2 p6
C2GC03
S S S S C
5' UTR
Pf3'
hDHFR
Pf3'
hDHFR
Py3'
BSD
Pf 3'
1 exons 2-13
pBS
non-functional pfcrt remnant (plasmid)
1
pBS
non-functional pfcrt remnant (plasmid)
1
pBS
non-functional pfcrt remnant (endogenous)
functional wild-type pfcrt
p7 p1/p4 p5 p2

Fig. S1 (previous page). Allelic replacement of *pfcrt* via two rounds of single-site crossover. **(A)** Allelic replacement of *pfcrt* in the CQS clone GC03. The primary transformation construct phDHFR-crt-GC03$^{Pf3'}$ (8.1 kb) used human dihydrofolate reductase (hDHFR) as the selectable marker and contained a *pfcrt* sequence (from GC03) that had a deletion in exon 1 and lacked the introns between exons 2-13. Transfection of GC03 with this construct led to the C1^{GC03} clone, which had undergone single-site crossover and homologous recombination upstream of codon positions 74-76. C1^{GC03} contained a functional *pfcrt* allele (unaltered at the polymorphic positions) that retained endogenous promoter and terminator elements. The putative transcription start site in the 5' untranslated region (UTR) upstream of the functional allele is indicated. Downstream *pfcrt* remnant sequences were truncated in exon 1, had a 5' in-frame stop codon to prevent translation and lacked a promoter. **(B)** Generation of lines expressing recombinant *pfcrt* variants containing entire sets of point mutations from CQR parasites. The secondary transfection constructs used blasticidin S-deaminase (BSD) as the selectable marker. The diagram illustrates transfection of the CQS clone C1^{GC03} with pBSD-crt-Dd2$^{Py3'}$ (7.7 kb). This construct contained a *pfcrt* sequence from Dd2 with a deletion in exon 1, no introns between exons 2-13 and a downstream 0.7 kb 3' UTR sequence from the *P. yoelii* ortholog *pycg10*. Homologous recombination upstream of codon positions 74-76 resulted in generation of a functional *pfcrt* allele containing all the point mutations from the CQR parasite Dd2, under the control of *pfcrt* 5' UTR and *pycg10* 3' UTR regulatory elements. This recombination event was isolated in the clone C4^{Dd2}. Downstream remnant *pfcrt* fragments were truncated in exon 1, had a 5' in-frame stop codon and lacked a promoter. The copy number of these remnant fragments depended on the number of tandem integrations of the hDHFR- or BSD-based constructs. Additional constructs that were used included pBSD-crt-Dd2$^{Pf3'}$, pBSD-crt-K76I$^{Pf3'}$and pBSD-crt-7G8$^{Py3'}$. Pf3' and Py3' constructs were 8.1 kb and 7.7 kb respectively. These constructs contained *pfcrt* sequences from the CQR lines Dd2 (Indochina), K76I (of Sudanese origin) and 7G8 (Brazil). Superscripts refer to the origin of the 3'UTR (Pf3', 1.1 kb fragment from *pfcrt*; Py3', 0.7 kb fragment from *pycg10*). **(C)** C3^{Dd2} and C4^{Dd2} differ in their 3' UTR. C5^{K76I} and C6^{7G8} (not shown) differ in the *pfcrt* coding sequence, which came from K76I and 7G8 respectively and which resulted in the expression of a distinct PfCRT haplotype. C2^{GC03} was generated from C1^{GC03} transformed with pBSD-crt-Dd2$^{Py3'}$. In C2^{GC03}, recombination occurred in the contiguous *hrp3* / pBluescript (pBS) region downstream of the functional *pfcrt* allele. This did not alter the *pfcrt* coding sequence and served as a critical internal control for phenotypic analysis. PfCRT haplotypes and primer details are listed in Tables 1 and S2 respectively. All sequences are drawn to scale except for pBS and the hDHFR and BSD selectable markers (all 3.0 kb). C, Cla I; S, Sal I; Pf3' and Py3' are from the 3' UTR regions of *pfcrt* and *pycg10*, respectively; ▬ and ▩ represent *pfcrt* sequences from the CQR line Dd2 and the CQS lines GC03 and C1^{GC03}, respectively.

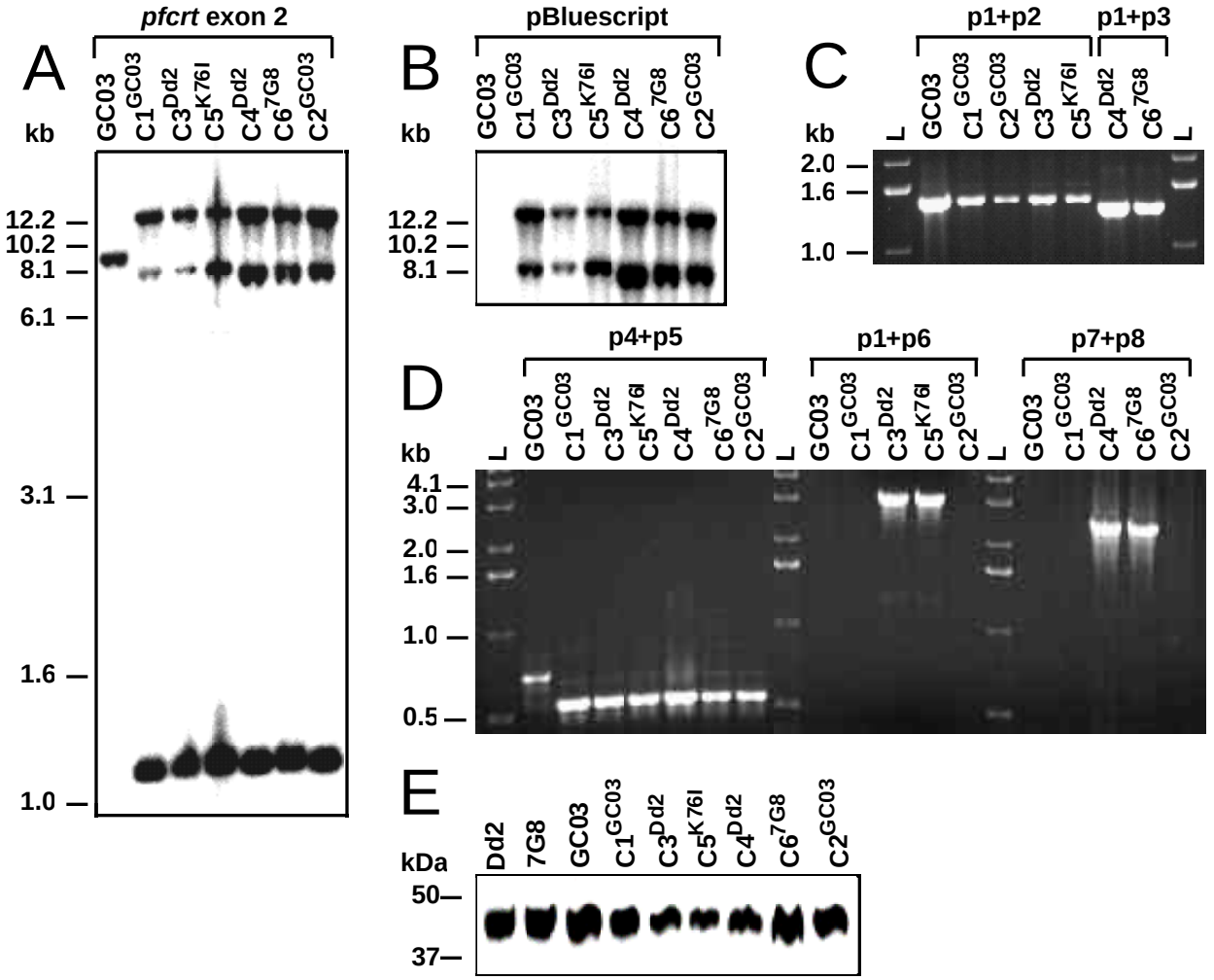

Fig. S2. Molecular confirmation of *pfcrt* allelic exchange and expression. Genomic DNA of recombinant and nontransformed lines was digested by Cla I + Sal I and hybridized with *pfcrt* exon 2 **(A)** or pBluescript **(B)** probes. Band patterns were consistent with plasmid integration into the *pfcrt* locus by homologous recombination. RT-PCR **(C)** and PCR **(D)** analysis confirmed transcription of the functional recombinant *pfcrt* allele and replacement of the endogenous *pfcrt* allele. No transcription was observed from the downstream remnant *pfcrt* sequences (Fig. S1, data not shown). Allelic replacement was confirmed by sequence analysis of PCR products (data not shown). Primer sequences and band sizes are listed in Table S1 (see separate file). **(E)** Western blot analysis revealed expression of full-length PfCRT in control and recombinant clones.

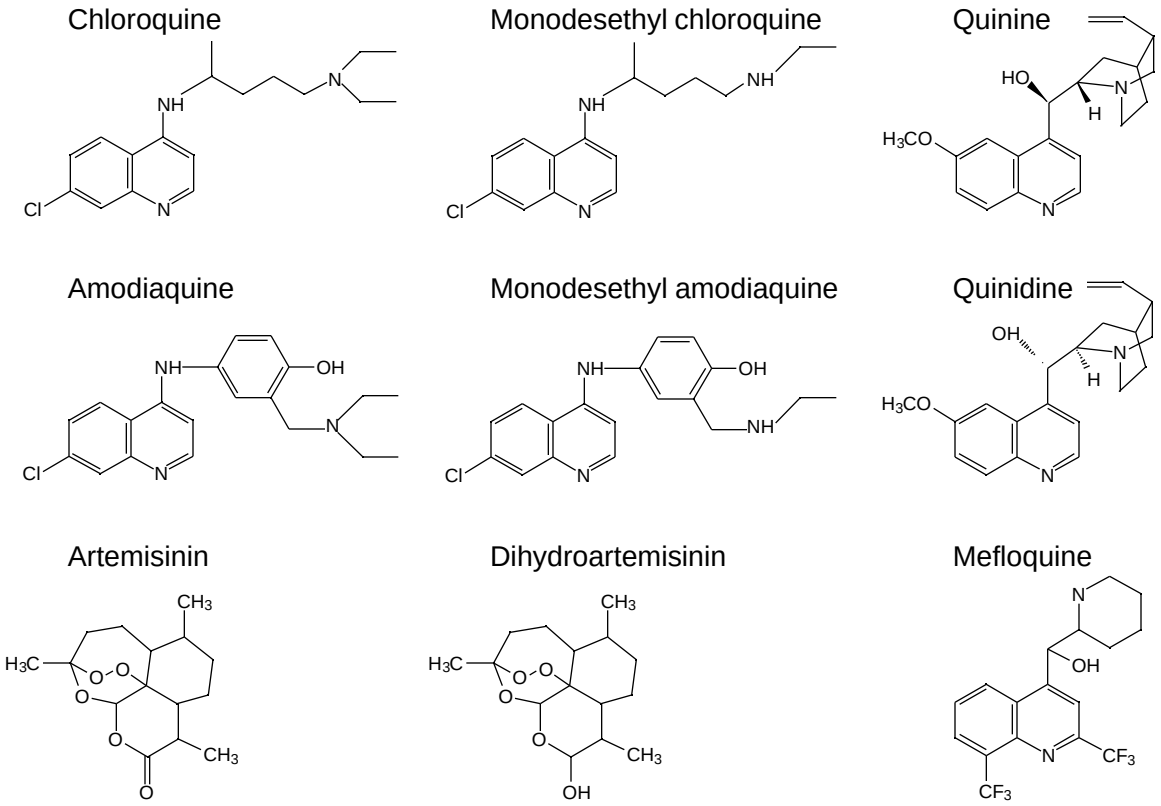

Fig. S3. Structure of antimalarial drugs and active metabolites tested against *pfcrt*-modified clones. Quinine, quinidine, and mefloquine (all quinoline methanols) share the aminoquinoline ring found in chloroquine and its side-chain analog amodiaquine, whereas this ring is absent in artemisinin (a sesquiterpene peroxide).

Table S1. Primer pairs used for the analysis of ***pfcrt*** allelic exchange events*

Clone	Nucleic Acid	p1+p2	p1+p3	p4+p5	p1+p6	p7+p8
GC03[†]	cDNA	1514 bp	negative	390 bp	negative	negative
	genomic DNA	3305 bp	negative	722 bp	negative	negative
$C1^{GC03}$	cDNA	1514 bp	negative	390 bp	negative	negative
	genomic DNA	1683 bp	negative	559 bp	negative	negative
$C2^{GC03}$	cDNA	1514 bp	negative	390 bp	negative	negative
	genomic DNA	1683 bp	negative	559 bp	negative	negative
$C3^{Dd2}/C5^{K76I}$	cDNA	1514 bp	negative	390 bp	negative	negative
	genomic DNA	1683 bp	negative	559 bp	3210 bp	negative
$C4^{Dd2}/C6^{7G8}$	cDNA	negative	1399 bp	390 bp	negative	2489 bp[§]
	genomic DNA	negative	1568 bp	559 bp	2850 bp	2658 bp

*p1: 5'-CCGTTAATAATAAATACACGCAG (pfcrt 5'UTR); p2: 5'-TCCTTATAAAGTGTAATGCGATAGC (Pf3');
p3: 5'-CATAGTTTGTATCTTTATGTGGCA (Py3'); p4: 5'-AATTCAAGCAAAAATGACGAGCG (pfcrt exon 1);
p5: 5'-GACTGAACAGGCATCTAACATGG (pfcrt exon 2); p6: 5'-ACAGCCGACGGCAGTTGGG (BSD);
p7: 5'-CTTTCCCAAGTTGTACTGCTTC (pfcrt 5'UTR); p8: 5'-CAGGATCCTATTTCAAAAATCTTAGCATAAGG (Py3').

[†] The same sizes were observed for Dd2, K76I and 7G8.

§ This predicted size was not tested by RT-PCR. Shaded cells indicate PCR reactions shown in Fig. S2C, D.

All other primer combinations were tested and matched predictions.

Table S2. Antimalarial drug responses in ***pfcrt-***modified ***P. falciparum*** lines

	Parasite Clones									
Drug Levels	GC03	C1^{GC03}	C2^{GC03}	C3^{Dd2}	C4^{Dd2}	Dd2	C5^{K76I}	K76I	C6^{7G8}	7G8
CQ IC_{50}	29.2±2.0	27.4±3.1	22.9±2.8	143.8±11.4	147.4±13.3	195.1±25.3	101.7±7.0	122.9±17.3	126.9±17.2	140.4±15.0
CQ IC_{90}	36.2±1.2	33.3±3.9	31.1±3.0	237.0±13.6	236.7±19.5	281.4±24.3	165.1±13.6	194.1±20.0	192.6±20.4	239.5±21.8
CQ IC_{50}/VP	28.7±2.3	27.9±2.8	21.8±2.6	76.2±7.5	71.3±9.1	70.4±12.3	49.4±4.9	57.8±10.5	106.2±11.7	103.4±10.6
CQ IC_{90}/VP	36.2±1.3	33.8±3.7	30.4±3.2	137.9±9.5	128.9±11.0	116.6±14.3	100.4±11.5	93.5±14.2	148.6±15.4	131.5±30.7
m-dCQ IC_{50}	35.3±1.4	nd	37.7±1.0	875.2±144.3	1182.2±72.2	2054.0±180.8	635.3±97.3	nd	649.4±37.7	948.8±86.3
m-dCQ IC_{90}	52.1±2.4	nd	67.3±2.8	1855.2±304.5	1900.8±159.7	3265.6±359.1	876.9±134.0	nd	1321.0±112.7	1725.7±78.4
ADQ IC_{50}	18.3±3.6	20.2±3.2	18.2±4.1	31.6±2.7	25.8±2.3	23.5±5.1	28.9±5.2	22.4±3.0	35.8±7.2	31.7±6.8
ADQ IC_{90}	23.1±4.7	24.7±3.3	22.7±4.7	43.5±1.3	36.0±4.2	35.5±7.9	37.4±7.4	27.9±4.1	45.6±7.6	47.5±6.4
ADQ IC_{50}/VP	18.2±2.3	19.2±2.1	18.1±3.4	24.5±0.6	21.0±2.3	20.9±1.3	22.6±3.4	23.6±4.8	27.5±4.5	25.9±2.9
ADQ IC_{90}/VP	20.8±1.5	24.3±4.7	24.9±1.3	35.4±4.3	31.8±2.5	36.2±2.4	38.5±4.7	36.6±7.5	38.1±7.1	38.3±3.3
m-dADQ IC_{50}	32.5±0.6	nd	45.2±9.7	70.2±3.3	67.9±2.0	96.7±19.9	54.8±1.2	nd	86.2±5.6	229.3±12.2
m-dADQ IC_{90}	49.6±4.8	nd	61.1±12.0	115.9±18.6	122.0±8.2	125.5±23.7	80.9±2.0	nd	154.0±2.5	291.5±22.1
QN IC_{50}	228.0±41.1	236.0±50.4	171.2±28.4	74.7±11.2	93.0±16.6	290.0±44.5	52.3±5.2	17.2±3.9	71.5±14.2	135.6±20.4
QN IC_{90}	773.3±136.3	727.6±161.7	501.1±139.8	270.6±53.9	446.4±96.2	537.0±65.7	169.6±14.6	73.4±18.8	285.6±49.6	310.0±53.5
QN IC_{50}/VP	219.8±32.5	220.4±48.4	169.8±27.3	29.9±4.0	36.0±7.5	87.8±18.3	24.1±2.5	42.1±10.5	55.0±7.1	104.3±22.6
QN IC_{90}/VP	755.8±150.0	704.1±180.1	474.6±115.2	161.4±43.7	530.9±148.9	276.8±55.2	201.8±36.1	139.0±32.8	237.3±46.3	272.2±53.9
QD IC_{50}	42.3±8.0	34.4±7.3	26.9±5.4	38.7±4.1	38.±4.6	178.3±22.3	32.5±6.1	64.2±13.2	21.5±3.3	44.9±10.3
QD IC_{90}	83.3±11.6	60.0±7.8	51.5±9.5	175.6±26.7	122.3±32.5	308.5±36.6	120.8±22.7	167.6±26.3	97.8±18.2	102.5±23.2
QD IC_{50}/VP	37.4±6.7	35.9±6.9	24.7±4.0	15.8±2.6	15.8±2.5	58.4±5.2	18.8±4.0	29.8±5.6	17.1±2.5	36.5±7.9
QD IC_{90}/VP	72.1±9.3	58.3±7.7	47.5±8.8	110.6±22.8	73.5±18.0	167.7±3.5	108.5±21.7	68.5±11.9	82.4±12.7	82.0±21.0
MFQ IC_{50}	52.6±5.4	59.1±6.9	54.7±1.5	24.1±2.2	33.1±3.1	46.8±2.0	30.9±3.5	26.8±6.8	27.3±3.4	9.6±1.3
MFQ IC_{90}	71.4±8.9	111.0±17.1	105.8±7.2	55.1±2.0	59.4±1.7	123.7±12.9	63.7±8.9	53.9±10.1	52.8±2.8	27.3±2.4
MFQ IC_{50}/VP	65.0±5.7	78.0±9.3	76.4±2.7	20.1±0.6	22.4±0.4	19.4±1.0	24.5±2.7	38.9±9.6	27.2±3.3	8.4±0.9
MFQ IC_{90}/VP	95.7±10.5	130.3±18.4	124.2±4.7	90.1±15.6	84.7±8.0	103.7±13.2	103.3±16.1	92.3±19.6	77.9±2.9	20.4±2.5

~ ***Continued*** ~

Table S2. Antimalarial drug responses in ***pfcrt-***modified ***P. falciparum*** lines (***continued***)

	Parasite Clones									
Drug Levels	GC03	C1^{GC03}	C2^{GC03}	C3^{Dd2}	C4^{Dd2}	Dd2	C5^{K76I}	K76I	C6^{7G8}	7G8
ART IC_{50}	39.4±6.9	39.2±6.2	39.1±7.0	12.0±1.2	12.6±1.8	46.3±7.6	15.8±3.5	30.6±3.1	17.2±3.0	21.6±6.3
ART IC_{90}	65.2±12.0	65.2±11.8	65.2±10.6	30.5±2.7	31.8±6.2	60.7±10.1	40.1±5.3	46.3±4.6	30.2±4.8	42.0±6.8
ART IC_{50}/VP	33.2±6.0	33.9±6.5	35.0±6.7	9.3±0.7	9.6±1.4	32.6±3.9	10.2±2.3	33.9±3.2	14.3±3.6	20.1±5.8
ART IC_{90}/VP	66.6±12.8	59.5±11.1	63.8±10.1	31.6±3.6	34.5±5.7	58.9±19.0	45.3±2.1	53.5±5.6	30.6±6.5	40.1±3.1
dhART IC_{50}	3.5±0.2	nd	4.6±0.3	1.7±0.1	2.3±0.5	4.6±0.7	1.6±0.1	nd	1.9±0.5	2.2±0.1
dhART IC_{90}	13.6±0.4	nd	14.9±0.2	5.5±0.7	10.7±3.0	14.9±1.2	9.0±1.3	nd	7.3±.14	7.0±1.6

IC_{50} and IC_{90} values were derived by curve fitting analysis of drug inhibition data generated from 72-hr [^{3}H]-hypoxanthine incorporation assays. All lines were tested at least four times in duplicate against each antimalarial compound, except the metabolites that were tested three times in duplicate. Values indicate mean ± SEM, shown in nM. ADQ, amodiaquine; ART, artemisinin; CQ, chloroquine; dhART, dihydroartemisinin; m-dADQ, mono-desethylamodiaquine; m-dCQ, mono-desethylchloroquine; MFQ, mefloquine; nd, not determined; QD, quinidine; QN, quinine; VP, verapamil (used at 0.8 µM).